Journal of Applied Polymer Science

Synthesis and Characterization of Bio-Based Thermosetting Resins from Lactic Acid and Glycerol

Fatimat Oluwatoyin Bakare,[1] Mikael Skrifvars,[1] Dan Åkesson,[1] Yanfei Wang,[2] Shahrzad Javanshir Afshar,[1] Nima Esmaeili[1]

[1]School of Engineering, University of Boras, Boras, Sweden

[2]University of South China, China

Correspondence to: D. Åkesson (E-mail: dan.akesson@hb.se)

ABSTRACT: A bio-based thermoset resin has been synthesized from glycerol reacted with lactic acid oligomers of three different chain lengths (*n*): 3, 7, and 10. Lactic acid was first reacted with glycerol by direct condensation and the resulting branched molecule was then end-functionalized with methacrylic anhydride. The resins were characterized by Fourier-transform infrared spectroscopy (FT-IR), by ^{13}C-NMR spectroscopy to confirm the chemical structure of the resin, and by differential scanning calorimetry and dynamic mechanical thermal analysis (DMTA) to obtain the thermal properties. The resin flow viscosities were also measured using a rheometer with different stress levels for each temperature used, as this is an important characteristic of resins that are intended to be used as a matrix in composite applications. The resin with a chain length of three had better mechanical, thermal, and rheological properties than the resins with chain lengths of seven and 10. Also, its bio-based content of 78% and glass transition temperature of 97°C makes this resin comparable to commercial unsaturated polyester resins. © 2014 Wiley Periodicals, Inc. J. Appl. Polym. Sci. **2014**, *131*, 40488.

KEYWORDS: biopolymers and renewable polymers; composites; crosslinking; resins; thermosets

Received 29 October 2013; accepted 17 January 2014

DOI: 10.1002/app.40488

INTRODUCTION

In recent years, renewable resources are increasingly providing sustainable platforms to substitute petroleum-based polymers. Many research projects have shown that bio-based resins from renewable resources can compete with or even surpass fossil fuel resources based on considerations related to cost and eco-friendliness.[1–4] The development of monomers or raw materials for these bio-based resins (for example: soybean oils, linseed oil, or lactic acid) can enable a reduction in the use of fossil resources.[5–7] These resins have been used in different applications such as paints, inks, coatings, soaps, and plasticizers.[5]

Lactic acid (2-hydroxypropanoic acid) is produced from the fermentation of renewable sources (e.g., carbohydrates) or by chemical synthesis.[1,8–10] It is widely used in the pharmaceutical, food, and chemical industries. The demand for lactic acid has grown because of its use in the synthesis of poly(lactic acid) (PLA), which is a biodegradable and biocompatible polymer, and it is used in many thermoplastics applications such as packaging products, biodegradable plastic products, and biomedical materials.[1,8–12]

For composite applications, however, thermosetting resins are often used because of their low viscosity, and therefore they are desirable for use as a bio-based composite matrix resin.[2,13,14] Much research has been performed on the preparation of thermosetting resins from lactic acid or lactides.[11,14–16] These poly(lactic acid) resins, produced by ring-opening polymerization, are used in biomedical applications, e.g., in the synthesis of ε-caprolactone (CL) and D, L-lactide to obtain telechelic star-oligomers.[17,18] The synthesis of poly(D,L-lactide-co-(ε-caprolactone)) reinforced with β-TCP and $CaCO_3$ for intervertebral disk augmentation[19] and the end-functionalization of polylactide with D-glucose and D-galactose for the development of micellar carrier systems[20] are examples of synthesis performed for drug-delivery applications. Other syntheses have also been performed for tissue-engineering applications (i.e., as a scaffold material to support cell and tissue growth),[21] packaging applications,[22] and coating applications.[11]

We have previously described a thermosetting resin prepared by direct condensation of pentaerythritol, itaconic acid, and lactic acid.[11] The star-shaped molecules obtained with pentaerythritol as the core molecule were end-capped with methacrylate groups. Thus, it was possible to crosslink the resin by free radical polymerization. This resin had relatively good mechanical properties, but it also had a relatively high viscosity.

The aim of this study has been to investigate the possibility of producing bio-based resin from lactic acid and glycerol. Glycerol and lactic acid were reacted in a direct condensation,

© 2014 Wiley Periodicals, Inc.

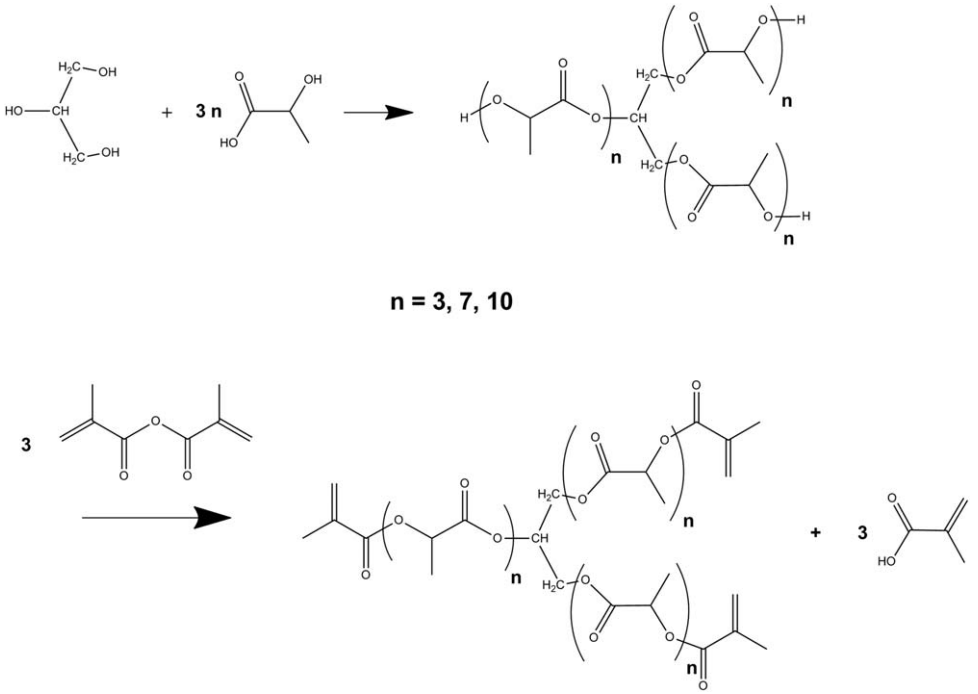

Figure 1. Reaction scheme for the two-stage synthesis of methacrylate functionalized glycerol–lactic acid resins with lactic acid chain lengths of $n = 3$, $n = 7$, and $n = 10$.

followed by end-functionalization with methacrylic anhydride (Figure 1). By varying the molar amount of lactic acid, it was possible to obtain resins with different glycerol–lactic acid branch length. The possible advantages of using glycerol as the core molecule instead of pentaerythritol are (1) that glycerol is generated as a by-product from biodiesel production[23–25] and, like lactic acid, is a renewable compound; and (2) that it is a cheap raw material[26–28] and it will yield molecules with only three branches, thereby lowering the molecular weight and reducing the viscosity of the resin produced. The influence of branch length was studied and the cured resins were characterized using DMTA, differential scanning calorimetry (DSC), and thermogravimetric analysis (TGA).

EXPERIMENTAL

Materials

L-lactic acid (88–92%; Sigma-Aldrich) and glycerol (99.5%; Scharlau, supplied by Fisher Scientific, Sweden) were used as the main reactants. Toluene was used as solvent (99.99%; supplied by Fisher Scientific) and methanesulfonic acid ($\geq$ 98%; Alfa Aesar) was used as the catalyst in the condensation reaction. Hydroquinone (99%; Acros Organics, supplied by Fisher Scientific) was used as inhibitor during the end-functionalization reaction. Methacrylic anhydride (94%; Alfa Aesar) was used as the reagent for the end-functionalization. Dibenzoyl peroxide, 2 wt %, was used as free radical initiator for crosslinking of the synthesized resin. All reactions were performed in an atmosphere of nitrogen.

Synthesis

The lactic acid was first evaporated in a rotary evaporator to remove the water content and was then stored dry at room temperature. The synthesis was performed in two stages. In the first stage (the condensation reaction stage), a star-shaped oligomer of glycerol and lactic acid was prepared. To study the influence of the length of the chains, three different chain lengths in the glycerol branches were used ($n = 3$, 7, and 10). This was performed by using 9, 21, and 30 moles of lactic acid for each mole of glycerol. In the second step, the resin was reacted further with methacrylic anhydride. The chemical reaction is shown in Figure 1.

Condensation Reaction of the Lactic Acid (First Stage of Synthesis)

Glycerol (0.12 mole) was added to 1.08 moles of lactic acid diluted in 50 g of toluene containing 0.1 wt % of methanesulfonic acid, which was used as catalyst. All components were placed in a three-necked round-bottom flask equipped with a magnetic stirrer, a nitrogen inlet, and an azeotropic distillation apparatus. The flask was heated for 2 h in an oil bath with a set temperature in the flask of 145°C under constant stirring. The water produced in the reaction was collected by azeotropic distillation. After the initial 2 h, the temperature was raised to 165°C for another 2 h, and then increased to 195°C for 1 h. The same procedure was used to prepare the thermoset resins with longer lactic acid branches ($n = 7$ and $n = 10$), where 2.52 moles and 3.6 moles of lactic acid were used, respectively.

End-Functionalization of the Oligomers (Second Stage of Synthesis)

The remaining reactant solution was cooled to 110°C and maintained at that temperature. As a stabilizer, hydroquinone (0.1 wt %) was then added to the reaction mixture with stirring, and 0.396 mole of methacrylic anhydride was added dropwise to the reaction

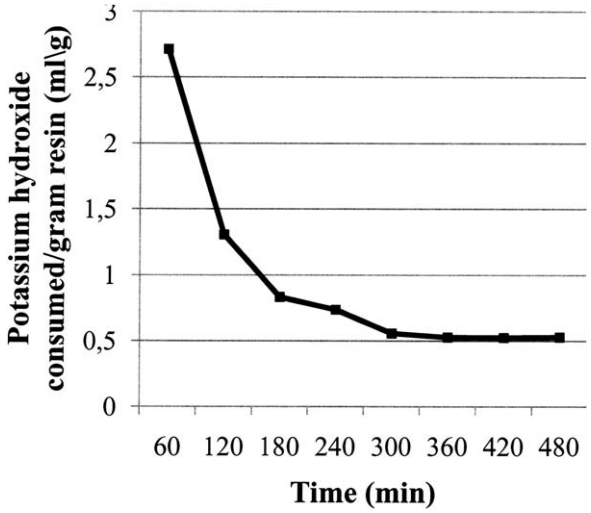

Figure 2. Potassium hydroxide consumption curve from acid–base titration.

mixture for 4 h, with constant stirring and in an atmosphere of nitrogen. The thermoset resins with $n = 7$ and $n = 10$ were prepared using the same method.

The residual methacrylic acid that had formed after the end-functionalization and also the toluene were removed by rotary evaporator distillation at a temperature of 60°C and pressure of 13 mbar to purify the resin before polymerization.

Curing of Resin

The thermal curing was performed by mixing the resin with dibenzoyl peroxide (2 wt %) as the initiator and *N*, *N*-dimethylaniline (0.5 wt %) as the accelerator. The sample mixture was left to cure at room temperature for 1 h. After this, it was placed in an oven to postcure at 150°C for 20 min. The cured sample was then analyzed using DMTA, DSC, TGA, and Fourier-transform infrared (FT-IR).

Characterization

To follow the progress of the condensation reaction, the reaction-conversion percentage was determined by titrating the carboxyl groups during the synthesis. One-gram samples were taken after reaction times of 1, 2, 3, 4, and 5 h. The sample was diluted with 20 mL of a 1 : 1 xylene/isopropyl alcohol solution and titrated with 0.5*M* KOH solution in absolute ethanol. A few drops of 1% phenolphthalein solution in ethanol were used as indicator and then the potassium hydroxide consumed was measured.

The resin synthesized from both the first stage and the second stage was examined using ^{13}C NMR (Chemagnetics CMX spectrometer) at 400 MHz. Samples were dissolved in $CDCl_3$. The average glycerol–lactic acid branch length and the degree of end-functionalization of the branches with methacrylic anhydride were calculated.

The neat and cured resins were analyzed using FT-IR spectroscopy on a Nicolet 6700 spectrometer (Thermo Fisher Scientific, MA). Resin synthesized during the first stage, resin after the second stage, and cured resin was analyzed by FT-IR.

The uncured and cured resins were also analyzed by DSC on a TA Instrument Q 1000 (supplied by Waters LLC, New Castle, DE). Samples were placed in sealed aluminum pans and heated from −20 to 200°C at a rate of 10°C/min in a nitrogen atmosphere. Data obtained from the first heating were used to investigate the crosslinking reaction efficiency.

Dynamic mechanical analysis (DMA Q800 from TA Instruments, supplied by Waters LLC), was performed on the cured resins and was run in the dual cantilever bending mode with a sample dimension of approximately 35 × 2 × 8 mm. The temperature ranged from −40 to 150°C with a heating rate of 3°C/min in an atmosphere of nitrogen; the frequency was 1 Hz and the amplitude was 15 μm.

TGA was performed on the cured resin (Q500 from TA Instruments, supplied by Waters LLC). A sample of about 20 mg was heated from 30 to 650°C at a heating rate of 10°C/min in a nitrogen purge stream.

The viscosity of the uncured resin was analyzed using a modular compact rheometer (Physica MCR 500). A truncated cone plate configuration was used for all measurements (1 mm, 25°C) and the analysis was run in rotational mode. Viscosities were measured at 25, 35, 45, 55, 70, and 100°C. For resin with $n = 3$, shear stress ranged from 0.5 to 2 Pa, while for resins with $n = 7$ and $n = 10$, the shear stress ranged from 100 to 2500 Pa and from 700 to 2500 Pa, respectively.

RESULTS

Titration

The degree of reaction was evaluated using an acid–base titration of the carboxylic groups present in the reaction mixture. As the reaction proceeds, the carboxylic groups react, which can be followed by titration with potassium hydroxide. The result is presented in Figure 2, where potassium hydroxide consumed decreases with increasing time up to 360 min, but there was no visible decrease in the consumption of potassium hydroxide thereafter up to 480 min. Thus, the condensation reaction proceeded until 360 min, and after the branch length did not increase due to opposing transesterification reactions.

^{13}C-NMR Spectroscopic Analysis

By ^{13}C-NMR analysis, it is possible to calculate the chain length of the lactic acid branches and to verify the end-capping reaction of the lactic acid branches with methacrylic acid. The ^{13}C-NMR spectrum of the carbonyl area (160–180 ppm) for the resin with $n = 3$ and not reacted with methacrylic anhydride is shown in Figure 3(a). The assignments of the peaks were performed with the help of previously reported data.[11,29,30]

The carbonyl peaks for the reacted lactic acid are similar to the carbonyl peaks for the lactic acid and pentaerythritol star-shaped resin[11] previously studied. The lactic acid gives two signals at 168.5–169.5 ppm (marked **A**), corresponding to carbonyl groups in the lactic acid branches, and also to carbonyl groups in lactic acid oligomers, not reacted with glycerol. The lactic acid end-group carbonyls are located at 173.5–174.5 ppm (marked **B**), and this signal includes both the glycerol–lactic acid branches and the lactic acid oligomers. These are signals

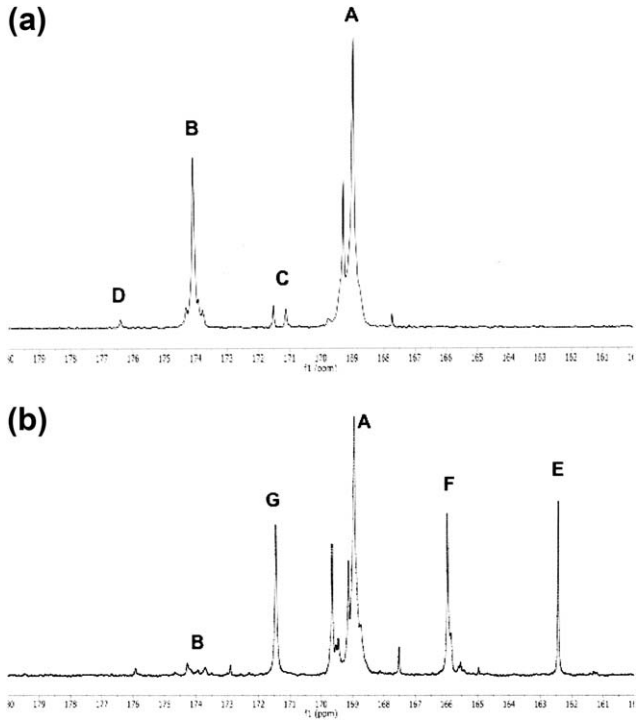

Figure 3. (a) Carbonyl area ^{13}C-NMR spectra for the glycerol–lactic acid resin with $n = 3$. (b) Carbonyl area ^{13}C-NMR spectra for the glycerol–lactic acid resin with $n = 3$ and end-group functionalized with methacrylic anhydride.

from the carbonyl group adjacent to the ester oxygen, while the carbonyls adjacent to the hydroxyl group give two smaller peaks at 171 and 171.5 ppm (marked **C**). A small signal for the carbonyl group in unreacted lactic acid can also be seen at 176.5 ppm (marked **D**).

From the carbonyl peak areas, it is possible to calculate the length of the glycerol–lactic acid branches, and both the percentage of lactic acid reacted with glycerol and the percentage of lactic acid reacted into free oligomers. The sum of the peak areas for all carbonyl signals is equivalent to the total amount of lactic acid units present in the resin, and the amount of lactic acid units reacted in the glycerol branches and in the free oligomers is equivalent to the sum of the areas for the two main peaks at 168.5–169.5 ppm and 173.5–174.5 ppm, subtracted with the area for the smaller peaks around 171–171.5 ppm. The peak area ratio gives the percentage of lactic acid reacted in the glycerol branches, and by doing a similar calculation the percentage of lactic acid in the oligomers can be calculated. The chain length of the glycerol branches is obtained from the ratio of the peak area corresponding to the total amount of lactic acid present in the branches divided by the peak area corresponding to lactic acid end-groups.

The spectrum for the methacrylic anhydride-modified glycerol–lactic acid resin is shown in Figure 3(b). The methacrylic anhydride end-group modification will result in three new carbonyl peaks, one for unreacted methacrylic anhydride at 162.5 ppm (marked **E**), one for reacted methacrylate ester at 166.0 ppm (marked **F**), and one for free methacrylic acid at 171.5 ppm (marked **G**). Unfortunately, it is not possible to distinguish between methacrylic anhydride reacted with the glycerol branches or the lactic acid oligomers, so these are both included in the peak at 162.5 ppm. Small peaks corresponding to still unreacted glycerol–lactic acid branches can be seen at 173.5–174.5 ppm (marked **B**), and the broad peak at 168.5–169.5 ppm (marked **A**)—corresponding to the lactic acid units in the branches and free oligomers—has been further broadened and split due to the adjacent methacrylate end-group. The percentage of glycerol–lactic acid chain ends reacted with methacrylic anhydride can be estimated from the peak area ratio for the peaks at 173.5–174.5 ppm and the peak at 166 ppm.

The ^{13}C-NMR spectra of the carbonyl area for the two other resins are shown in Figures 4 and 5. The assignments and markings are the same as in Figure 3. From the spectra for the resins not reacted with methacrylic anhydride, it can be seen clearly that the length of the glycerol–lactic acid branches are increased in the order expected, with the longest branch length for the resin with $n = 10$. The amount of methacrylic acid reacted with lactic acid ends are decreases with increasing branch length, which is to be expected, as the amount of end-groups is lower, and therefore the reaction probability is also lower. The branch lengths, percentage of lactic acid reacted, and the percentage of chain ends reacted for all resins are summarized in Table I.

FT-IR Spectroscopic Analysis

The FT-IR spectra were used to verify the resin functionalization with methacrylic anhydride in the second step by comparing them to the resin spectra from the first step. The cured resin was also analyzed to verify the curing reaction from the

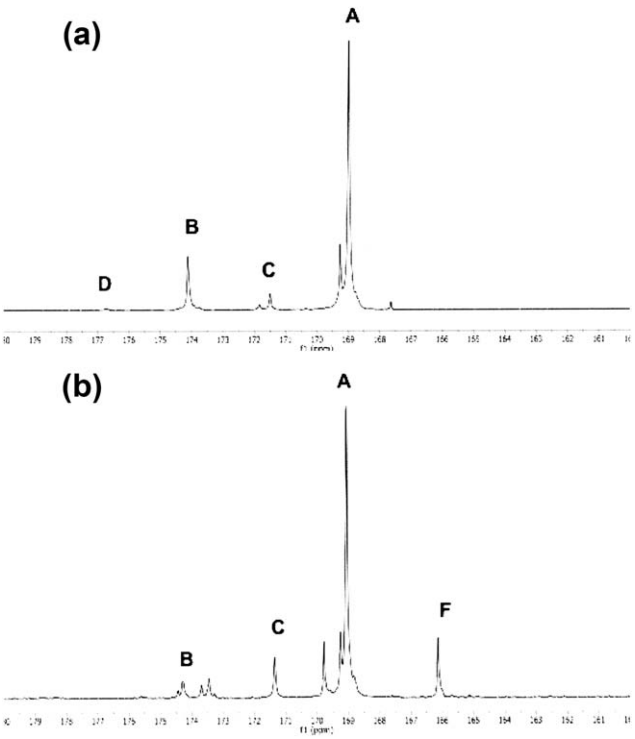

Figure 4. (a) Carbonyl area ^{13}C-NMR spectra for the glycerol–lactic acid resin with $n = 7$. (b) Carbonyl area ^{13}C-NMR spectra for the glycerol–lactic acid resin with $n = 7$ and end-group functionalized with methacrylic anhydride.

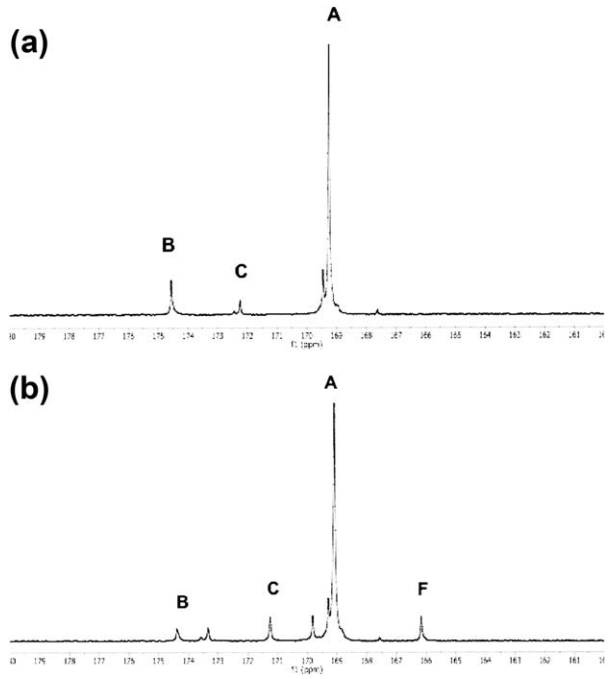

Figure 5. (a) Carbonyl area ^{13}C-NMR spectra for the glycerol–lactic acid resin with $n = 10$. (b) Carbonyl area ^{13}C-NMR spectra for the glycerol–lactic acid resin with $n = 10$ and end-group functionalized with methacrylic anhydride.

spectral bands corresponding to the carbon–carbon double bonds. In Figure 6(a), the spectrum for the uncured resin with $n = 3$ shows carbon–carbon double bonds at about 1640 cm^{-1} (stretching, C=C) and at 816 cm^{-1} (bending, $=CH_2$)[31]; this band was not present in the resin from the first step. This indicates that end-functionalization by methacrylic anhydride did occur. The disappearance of the carbon–carbon double bond peak and an increase in the band –CH stretch at about 2900 cm^{-1} in the cured resin[4,23] indicates that the crosslinking reaction of the resin had occurred. The complete crosslinking reaction was verified as shown in Figure 6(a); for the cured $n = 3$ resin, the spectrum shows no band at 1640 cm^{-1} and this clearly indicates that all double bonds had reacted when crosslinked. The almost complete disappearance of an absorbance at 3500 cm^{-1} after reaction with methacrylic anhydride indicates that almost all of the hydroxyl groups were reacted. The same results occurred with $n = 7$ resin and $n = 10$ resin as in Figure 6(b,c), but there was a decrease in reaction compared to the resin with $n = 3$.

Bio-Based Content

The bio-based content of the resins with $n = 3$, 7, and 10 was calculated using the ASTM D6866 standard according to the formula:

$$\text{Bio-based content} = \frac{\text{bio-based carbon content}}{\text{total carbon content}} \times 100$$

For the synthesized resins, the bio-based content is as follows:

$$\text{Bio-based content} = \frac{[G_m + 3n(L_m - W_m)]}{G_m + 3[(\text{MA}_m - M_m) + n(L_m - W_m)]}$$

Here, G_m is the weight of glycerol, n is the chain length, L_m is the weight of lactic acid, W_m is the weight of the water condensed, MA_m is the weight of methacrylic anhydride, and M_m is the weight of the methacrylic acid formed.

The calculation gives a bio-based content of 78% ($n = 3$), 89% ($n = 7$), and 92% ($n = 10$), respectively. This shows that a longer lactic acid chain length in the resin will give an increase in the bio-based content of the resin.

DSC Analysis

DSC was used to investigate the crosslinking reaction efficiency of the resins, by detecting any residual exothermal heat present in the cured and uncured specimens. The cured resins showed no exothermic peak for the samples, indicating that the three resins were fully cured. The uncured resins showed (as indicated in Figure 7) that the resin with $n = 3$ had a much higher exothermic heat evolved at 227.4 J/g than the resins with $n = 7$ and $n = 10$, which had exothermic heat evolved at 162.2 and 94.3 J/g, respectively, as listed in Table II. This is expected and

Table I. Summary of the ^{13}C-NMR Results

	Resin ($n = 3$)	Resin ($n = 7$)	Resin ($n = 10$)
% LA reacted with glycerol	90.2	84.7	87.2
% LA reacted into LA oligomers	8.9	14.1	11.9
% LA as lactide	0.9	1.1	1.0
Chain length of glycerol + LA polymer	4.0	9.2	13.0
Chain length of LA oligomers	2.2	2.6	2.8
	Resin ($n = 3$)	Resin ($n = 7$)	Resin ($n = 10$)
Reaction with MA:	+MA	+MA	+MA
% ends reacted (both glycerol + LA and poly(lactic acid)) ends	82.6	66.9	57.3
% free MA (as a % of the total MA present)	36.8	44.6	52.6
% free MA anhydride (as % MA of total MA)	20.9	-	

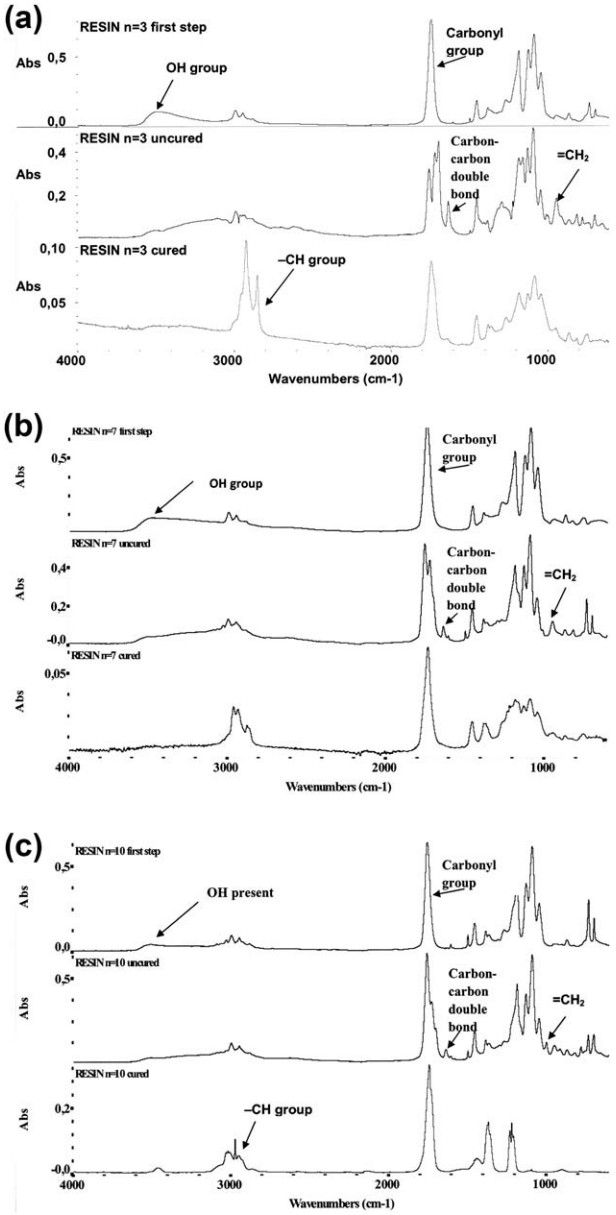

Figure 6. (a) FT-IR spectra of uncured and cured glycerol–lactic acid resin with $n = 3$. (b) FT-IR spectra of uncured and cured glycerol–lactic acid resin with $n = 7$. (c) FT-IR spectra of uncured and cured glycerol–lactic acid resin with $n = 10$.

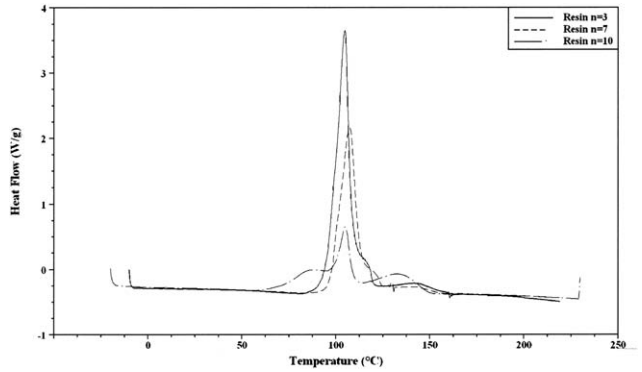

Figure 7. DSC curve for uncured glycerol–lactic acid resins with $n = 3$, $n = 7$, and $n = 10$.

Chang et al.[14] came to a similar conclusion. From the results, the resin with $n = 3$ with the highest exothermic heat and shortest arm length has a greater degree of reactivity than corresponding resins with $n = 7$ and $n = 10$.

DMA

The DMA was performed to characterize the viscoelastic properties of the cured resins. Figure 8(a) shows the storage modulus, G', for the resins with $n = 3$, $n = 7$, and $n = 10$, and for commercial polyester resin (CPR). G' was approximately 4314, 3766, 1736, and 2956 MPa, respectively, at 25°C. G', which is related to the polymer chain packing density in the glassy state, increased with decreasing lactic acid chain length of the resin. This agrees with the free volume theory, which states that with increasing crosslinking density there is a decrease in the free volume of the chain segments.[14] This can be explained by the fact that a shorter lactic acid chain length will give a higher crosslinking density. From Figure 8(a), it can also be concluded that the resins with $n = 3$ and $n = 7$ showed better polymer chain packing due their higher G' in the glassy state, compared to the CPR. Within the temperature range 50–80°C, there was a decrease in the G' due to the free movement of the polymeric chain, which is called the rubbery plateau region. According to Chang et al.,[14] this region becomes broader as the temperature increases when there is a decrease in the chain length of the oligomer, which indicates a denser and more restricted network. The resin with $n = 3$ is comparable to the CPR, since their behaviors were found to be almost the same in the rubbery region.

Table II. Characterization Results of the Resins

	DSC		DMA				TGA		
Resin	Heat of exotherm for uncured resin (J/g)	Heat of exotherm for cured resin (J/g)	T_g (°C)	Standard deviation	Storage modulus (MPa) at 25°C	Loss modulus (MPa) at 25°C	Degradation temperature at 10 wt % loss (°C)	Maximum degradation (°C)	Second derivative peak (°C)
n =3	227.4	0	97	352	4314	353.8	258	375	438
n =7	162.2	0	80	215	3766	228.6	248	366	436
n =10	94.3	0	54	59	1736	481.8	202	357	433

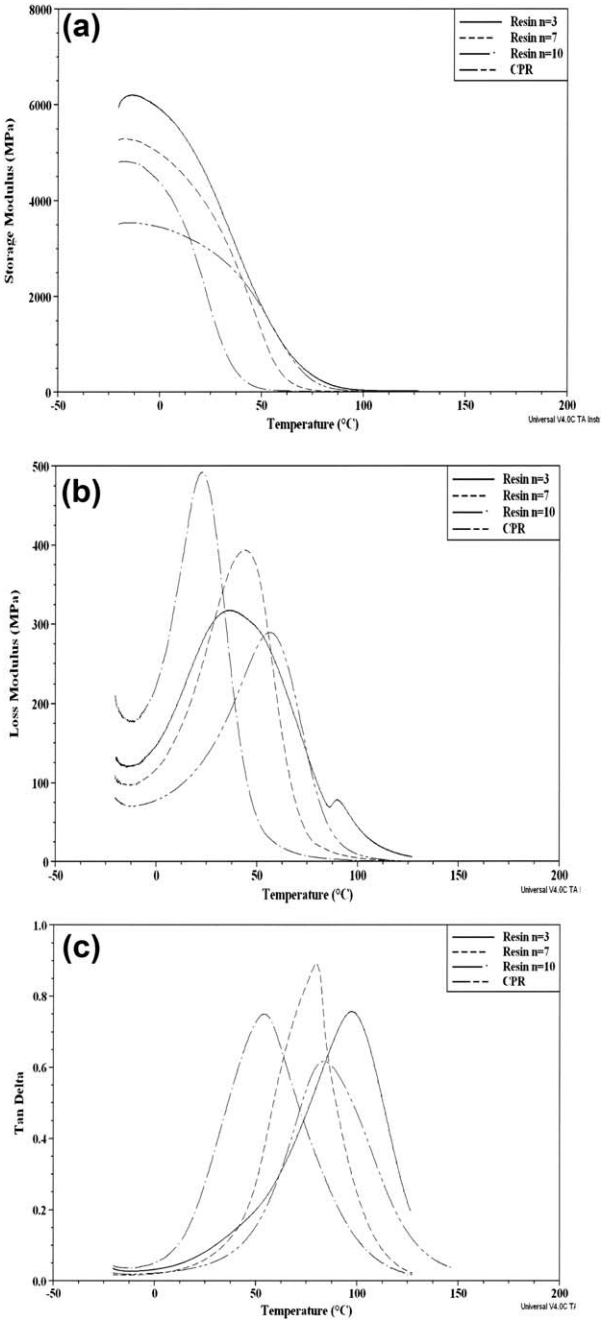

Figure 8. (a) DMA curve (storage modulus) for the crosslinked resin with $n = 3$, $n = 7$, and $n = 10$, and a commercial polyester resin (CPR). (b) DMA curve (loss modulus) for the crosslinked resin with $n = 3$, $n = 7$, and $n = 10$, and a commercial polyester resin (CPR). (c) DMA curve (tan δ) for the crosslinked resin with $n = 3$, $n = 7$, and $n = 10$, and a commercial polyester resin (CPR).

Figure 8(b) shows the temperature dependence of loss modulus G'', with the formation of a highly cross-linked network for the cured resins with $n = 3$, $n = 7$, and $n = 10$ and for the CPR. The G'' becomes broader and decreases in height with reduced chain length of the oligomer, due to increase in crosslinking density.[14] The low value of the G'' above the glass transition temperature was due to the rubbery plateau state of the cured resins, which means that according to the theory of rubber elasticity, the energy required to displace the network is reversible; so, the higher the crosslinking density, the stronger the reversibility tendency. Thus from Figure 8(b), the decrease in the peak value of the G'' occurs with decreasing chain length due to higher crosslinking density. Figure 8(c) shows the glass transition temperature measured as the peak of tan δ for the resins with $n = 3$, $n = 7$, and $n = 10$ and also the CPR, where the tan δ was recorded as 97, 80, 54, and 83°C, respectively. These results were to be expected, since shortening of chain length will increase the crosslinking density. Thus, the glass transition temperature will increase. From the FT-IR and DSC results, it was confirmed that all the resins were fully cured, so the decrease in T_g was due to the matrix rigidity. The increase in T_g and G' of the resin with $n = 3$ indicates a high degree of crosslinking, causing an increase in the stiffness of the network structure. From the figure, the glass transition temperature of resin with $n = 3$ was higher than the glass transition temperature of the CPR, and it was almost similar to the glass transition temperature of CPR in the literature.[31] But, in the case of resins with $n = 7$ and $n = 10$, the glass transition was found to be lower for this bio-based resin, which indicates that a lower degree of crosslinking and a less dense network was obtained.

TGA of the Cured Resins

The TGA was performed to investigate the thermal resistance of the resins by recording the percentage weight loss of the cured samples. This was performed to determine whether the influence of chain length affects the thermal resistance of the resin. The samples were heated at a uniform rate from 30 to 650°C. The thermogravimetric curves in Figure 9 show that the cured resin with $n = 3$ was relatively stable up to 240°C. At about 258°C, the resin lost 9.83 wt %, and at about 442°C, it had lost 89.34 wt %. Maximum amount of degradation occurred at 375°C. At 438°C, the curve of the derivative weight has a second peak. The cured resin with $n = 7$ was relatively stable up to 200°C. At about 248°C the resin lost 9.98 wt %, and at about 438°C, it had lost 90.47 wt %. The maximum amount of degradation occurred at 366°C. At 436°C, the curve of the derivative weight has a second peak. The cured resin with $n = 10$ was relatively stable up to 100°C. At about 202°C, the resin lost 9.92 wt %, and at about 429°C, it had lost 90.05 wt %. Maximum amount of degradation occurred at 357°C. At 433°C, the curve of the derivative weight has a second peak. Chang et al.,[14] who prepared a star-shaped oligomer of lactic acid, also agree that shorter arm lengths with higher crosslinking improve the thermal stability of PLA, which also leads to increase in the initial and final thermal degradation temperature. The thermal degradation temperature therefore has the tendency to increase with decreasing arm length of the star-shaped oligomers. From the results stated above, the fact that resin with $n = 3$ has a higher thermal degradation temperature indicates a higher crosslinking density, to improve its heat resistance capability compared to resin with $n = 7$ and $n = 10$.

Viscosity Measurement

The flow viscosity of a thermoset resin is of importance regarding how the resin can be processed. It was monitored using stress viscosimetry at temperatures of 25, 35, 45, 55, 70,

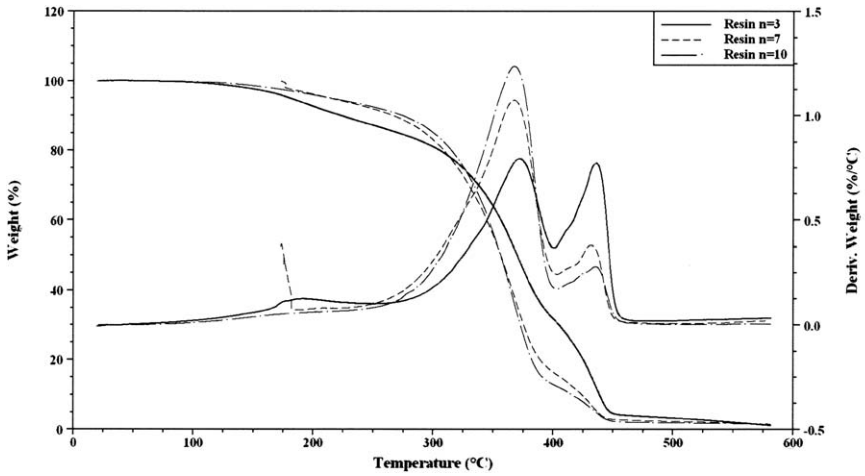

Figure 9. TGA curve for the cured resins with $n = 3$, $n = 7$, and $n = 10$.

and 100°C. In Figure 10, the graph shows that at room temperature the resin with $n = 3$ has a lower viscosity than the other two resins ($n = 7$ and $n = 10$), at 1.09 Pas. Upon heating to a temperature of about 100°C, the viscosity dropped to 0.0361 Pas for the resin with $n = 3$, to 0.3336 Pas for the resin with $n = 7$, and to 1.05 Pas for the resin with $n = 10$. The graph shows that the resins with $n = 7$ and $n = 10$ have a high viscosity, which would make the impregnation of resin into the fiber reinforcement difficult even at high temperatures. However, for the resin with $n = 3$ the viscosity found shows that it would be better suited for processing at higher temperatures than resins with $n = 7$ and $n = 10$. In a previous report,[11] where a four-armed, star-shaped oligomer was synthesized by reacting pentaerythritol with lactic acid, the viscosity was about 7000 Pas at room temperature and upon heating to 80°C it decreased to 4 Pas. The resin was only suited to processing at higher temperatures or to dilution with a reactive monomer; but comparing it to the viscosity of resin with $n = 3$ at room temperature—which was found to be 1.09 Pas—this novel resin clearly had better processability. It may be suited to processing at room temperature.

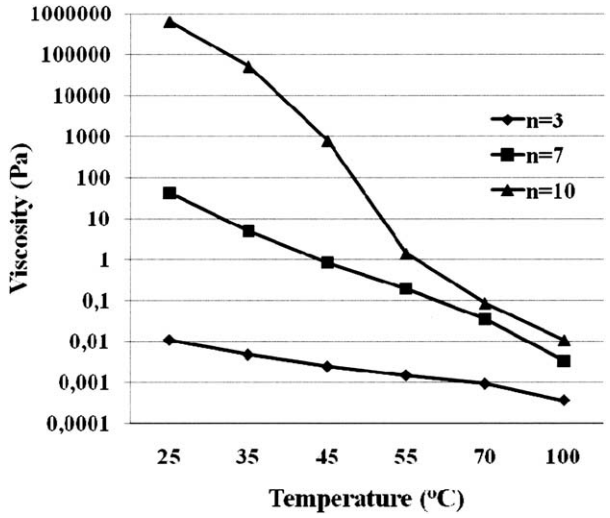

Figure 10. Viscosity of resins with $n = 3$, $n = 7$, and $n = 10$ as a function of temperature.

CONCLUSIONS

Bio-based thermoset resins of three types with chain lengths of three, seven, and 10 were synthesized from lactic acid in two synthesis stages. The first stage involved the direct condensation of lactic acid with glycerol; in the second stage, the glycerol–lactic acid oligomers obtained were reacted using methacrylic anhydride to obtain an unsaturated lactic acid polyester. This synthesis is straightforward and relatively cheap, due to the use of renewable reactants with good availability, and the synthesis could therefore be scaled up for industrial production.

This study shows that the glycerol–lactic acid resin with a lactic acid branch length corresponding to $n = 3$ has a calculated bio-based content of 78%, which is lower than for the resins with lactic acid lengths corresponding to $n = 7$ and $n = 10$, but it shows better mechanical and rheological properties. The glass transition temperature of $n = 3$ resin is 97°C, which is higher than for thermoplastic PLA and for commercial polyester resin.

The resin with $n = 3$ has a much lower flow viscosity at room temperature than the resins with $n = 7$ and $n = 10$, and upon heating to 70°C the viscosity drops much lower—which makes it good for impregnation into fibers both at lower temperatures and at increased temperatures. Whereas the resins with $n = 7$ and $n = 10$ were too viscous at lower temperatures and at increased temperatures, the viscosity become lower and they might still need to be diluted with reactive solvent to reduce the viscosity for impregnation. This could obviously be advantageous in the commercial production of bio-based resin because the viscosity allows easy impregnation into fiber; it will also give material with good mechanical properties that is prepared mainly from renewable materials. The mechanical properties when the resin is reinforced with fiber will be reported in a future publication.

ACKNOWLEDGMENTS

The NMR analysis and interpretation of spectra were performed by Andrew Root, Magsol, Finland.

REFERENCES

1. Adekunle, K.; Åkesson, D.; Skrifvars, M. *J. Appl. Polym. Sci.* **2010**, *115*, 3137.
2. Vigueras-Santiago, E.; Lopez Tellez, G.; Hernandez-Lopez, S. *Superficies y Vacio* **2009**, *22*, 5.
3. Del Rio, E.; Lligadas, G.; Ronda, J. C.; Galia, M.; Cadiz, V. *J. Appl. Polym. Sci.* **2010**, *48*, 5009.
4. Öztürk, C.; Küsefoğlu, S. H. *J. Appl. Polym. Sci.* **2010**, *118*, 3311.
5. Åkesson, D.; Skrifvars, M.; Lv, S.; Shi, W.; Adekunle, K. *Prog. Org. Coat.* **2010**, *67*, 281.
6. Ronda, J. C.; Lligadas, G.; Galia, M.; Biermann, U.; Metzger, J. O. *J. Appl. Polym. Sci.* **2006**, *44*, 634.
7. Eren, T.; Kusefoglu, S. H. *J. Appl. Polym. Sci.* **2005**, *97*, 2264.
8. Shen, Y.; Zhang, S.; Li, H.; Ren, Y.; Liu, H. *Chem. Eur. J.* **2010**, *16*, 7368.
9. Jamshidian, M.; Tehrany, E. A.; Imran, M.; Jacquot, M.; Desobry, S. *Compr. Rev. Food Sci. F.* **2010**, *9*, 552.
10. Datta, R.; Henry, M. *J. Chem. Technol. Biot.* **2006**, *81*, 1119.
11. Åkesson, D.; Skrifvars, M.; Seppälä, J.; Turunen, M.; Martinelli, A.; Matic, A. *J. Appl. Polym. Sci.* **2010**, *115*, 480.
12. Gil, M. H.; Marques, D. S.; Baptista, C. M. S. G. *J. Appl. Polym. Sci.* **2012**, *1*, E283.
13. Åkesson, D.; Skrifvars, M.; Seppälä, J.; Turunen, M. *J. Appl. Polym. Sci.* **2011**, *119*, 3004.
14. Chang, S.; Li, C. Z. J.; Ren, J. *Polym. Int.* **2012**, *61*, 1492.
15. Helminen, A. O.; Korhonen, H.; Seppälä, J. V. *J. Appl. Polym. Sci.* **2002**, *86*, 3616.
16. Sakai, R.; John, B.; Okamoto, M.; Seppälä, J. V.; Vaithilingam, J.; Hussein, H.; Goodridge, R. *Macromol. Mater. Eng.* **2013**, *298*, 45.
17. Helminen, A. O.; Korhonen, H.; Seppälä, J. V. *Macromol. Chem. Phys.* **2002**, *203*, 2630.
18. Helminen, A. O.; Korhonen, H.; Seppälä, J. V. *J. Appl. Polym. Sci.* **2003**, *41*, 3788.
19. Lopez, A.; Persson, C.; Hilborn, J.; Engqvist, H. *J. Biomed. Mater. Res. B Appl. Biomater.* **2010**, *95B*, 75.
20. Bernard, K.; Degee, P.; Dubois, P. *Polym. Int.* **2003**, *52*, 406.
21. Tang, M.; Haider, A. F.; Minelli, C.; Stevens, M. M.; Williams, C. K. *J. Appl. Polym. Sci.* **2008**, *46*, 4352.
22. Puaux, J. P.; Banu, I.; Nagy, I.; Bozga, G. *Macromol. Symp.* **2007**, *259*, 318.
23. Thompson, J. C.; He, B. B. *Appl. Eng. Agric.* **2006**, *22*, 261.
24. Pachauri, N.; He, B. In ASABE Annual International Meeting (American Society of Agricultural and Biological Engineers), Oregon Convention Center Portland, Oregon, **2006**, 1.
25. Thanh, L. T.; Okitsu, K.; Boi, L. V.; Maeda, Y. *Catalysts*, **2012**, *2*, 191.
26. Kim, S. C.; Kim, Y. H.; Lee, H.; Yoon, D. Y.; Elsevier, B. K. S. *J. Mol. Catal. B-Enzym.* **2007**, *49*, 75.
27. Mamiński, M.; Parzuchowski, P.; Borysiuk, P.; Boruszewski, P. In 2nd International Conference on Environmental Engineering and Applications (IPCBEE, Singapore), **2011**; Vol. *17*, p 13.
28. Da Silva, G. P.; Mack, M.; Contiero, J. *Biotechnol. Adv.* **2009**, *27*, 30.
29. Hiltunen, K.; Härkönen, M.; Seppälä, J. V.; Väänänen, T. *Macromolecules* **1996**, *29*, 8677.
30. Espartero, J. L.; Rashkov, I.; Li, S. M.; Manolova, N.; Vert, M. *Macromolecules* **1996**, *29*, 3535.
31. Hisham, S. F.; Ahmad, I.; Daik, R.; Ramli, A. *Sains Malays.* **2011**, *40*, 729.